

Lung diseases identification using hybrid transfer learning and bidirectional long short-term memory

Denis Eka Cahyani¹, Lucky Tri Oktoviana¹, Mohamad Yasin¹, Sapti Wahyuningsih¹, Dionixius¹, Ranti Maulidaningsih¹, Samsul Setumin²

¹Department of Mathematics, Faculty of Mathematics and Natural Sciences, Universitas Negeri Malang, Malang, Indonesia

²Centre for Electrical Engineering Studies, Department of Electrical Engineering, Faculty of Electrical Engineering, Universiti Teknologi MARA, Cawangan Pulau Pinang, Malaysia

Article Info

Article history:

Received Aug 8, 2024

Revised Oct 29, 2024

Accepted Nov 19, 2024

Keywords:

Bidirectional long short-term memory

Chest X-Ray

Convolutional neural network

Lung diseases

Resnet50

ABSTRACT

Lung diseases rank as the third most prevalent cause of mortality globally. Accurate identification of lung disease is essential to provide appropriate medical intervention for patients. This research devised a categorization system for lung diseases using chest X-Rays (CXR). The system can identify bacterial pneumonia, viral pneumonia, COVID-19, tuberculosis, and normal CXR. The approach for detecting lung diseases utilize a combination of hybrid transfer learning and bidirectional long short-term memory. The research included convolutional neural network (CNN) models including Resnet50-BiLSTM, VGG19-BiLSTM, InceptionV3-BiLSTM, Resnet50, VGG19, and InceptionV3. The Resnet50-BiLSTM model outperforms other models in terms of accuracy and overall performance. The Resnet50-BiLSTM model achieved an accuracy of 99.87%. The models that achieve the second greatest accuracy are Resnet50, VGG19-BiLSTM, VGG19, InceptionV3-BiLSTM, and InceptionV3. The research utilizes precision, recall, and F1-Measure to demonstrate that Resnet50-BiLSTM outperforms other methods by achieving the greatest value. This research improves the performance outcomes when compared to earlier studies.

This is an open access article under the [CC BY-SA](https://creativecommons.org/licenses/by-sa/4.0/) license.



Corresponding Author:

Denis Eka Cahyani

Department of Mathematics, Faculty of Mathematics and Natural Sciences, Universitas Negeri Malang St. Semarang No.5, Sumber Sari, Lowokwaru, Malang, East Java 65145, Indonesia

Email: denis.eka.cahyani.fmipa@um.ac.id

1. INTRODUCTION

The lungs are one of the organs that play an important role in the human respiratory system. Lung disease is a common disease and the third leading cause of death in the world [1]. According to WHO, lung diseases that have caused the most deaths in the world are pneumonia, tuberculosis (TB), and COVID-19 with around 450 million people affected [2]. The identification of lung diseases is important to provide appropriate medical intervention and prevent further spread. Efficient and precise screening methods may assist healthcare professionals in managing lung diseases [3].

Early detection of lung diseases involving pneumonia, TB, and COVID-19 could be achieved by many methods, including radiological assessment utilizing chest X-Ray (CXR) images or chest CT [4]. The diagnosis of patient diseases based on apparent signs of disease in CXR images is currently examined manually by doctors or health workers, resulting in a time-consuming process [5]. Conversely, the present advancement of deep learning has the capability to efficiently handle substantial volumes of data inside a little duration [6]. This study aims to use deep learning techniques to accurately identify lung diseases, including pneumonia, TB, and COVID-19, through processing CXR images.

Prior research has established the use of deep learning techniques for the identification of lung diseases using CXR images. Convolutional neural networks (CNN) are extensively used deep learning models for diagnosis of illness [7], [8]. Prior research has constructed CNN architectures, such as Resnet50 [9], [10], VGG19 [11], and Xception [12], for the purpose of identifying pneumonia in CXR images. Moreover, prior research has used ResNet [13], EfficientNet [14], and DenseNet [15] to identify TB, whereas InceptionV3 [16], ResNet [17], [18], and VGGNet [19] have been utilized for COVID-19 detection. The CNN models used in these investigations are transfer learning models specialized in the identification of a single form of lung illness, such as only pneumonia or merely COVID-19. CNN models have the ability to acquire localized responses from image data, enabling them to extract local data characteristics simultaneously. However, CNN encounters difficulties when it comes to processing pertinent spatiotemporal information (location and time) inside an image [20]. This constraint hinders CNN from effectively capturing the overall characteristics of picture data, rendering them unsuitable for learning the sequential correlation of data [21].

The bidirectional long short-term memory (BiLSTM) is another deep learning model that could successfully solve the drawbacks of CNN. BiLSTM is advantageous for sequential data modelling, however it lacks the ability to extract data features simultaneously [22]. The innovation of this study is in the use of a novel mix of CNN and BiLSTM transfer learning models, resulting in the creation of more precise and accurate models. In addition, this study integrates many lung diseases, including pneumonia, TB, and COVID-19, into a single detection method to enhance its effectiveness. Other investigations just identify COVID-19, pneumonia, and normal cases. However, this study aims to integrate TB data in order to increase the size and complexity of the research dataset. This study suggests the integration of CNN and BiLSTM models for the purpose of developing lung illness detection systems, namely for pneumonia, TB, and COVID-19.

The aim of this investigation is to enhance the identification of lung diseases (such as pneumonia, TB, and COVID-19) by using a novel fusion of CNN and BiLSTM transfer learning models on CXR pictures. The study will use a composite CNN transfer learning model consisting of Resnet50, VGG19, InceptionV3, and Xception. The novel fusion of CNN and BiLSTM transfer learning models is anticipated to speed up and improve the detection of lung illness with greater precision.

2. MATERIAL AND METHODS

This research provided a classification of lung diseases based on X-ray images. The classification model in this research was constructed by combining CNN and BiLSTM. The study methodology comprises the following steps: data pre-processing, data modelling, hyperparameter modification, and model evaluation. The evaluation approach employs a confusion matrix to compute metrics like as accuracy, precision, recall, and F1-Measure [23].

2.1. Dataset

This research utilizes a compilation of datasets sourced from several websites, including CXR images of COVID-19, normal cases, viral pneumonia cases [24], [25], CXR images of bacterial pneumonia cases [26], and CXR images of TB cases [27]. The collection has five distinct kinds of CXR images, namely bacterial pneumonia, viral pneumonia, COVID-19, tuberculosis, and normal. Figure 1 illustrates a sample CXR image from the dataset. Figure 1(a) displays a sample of bacterial pneumonia CXR, Figure 1(b) exhibits a sample of viral pneumonia CXR, Figure 1(c) presents a sample of COVID-19 CXR, Figure 1(d) illustrates a sample of tuberculosis CXR, and Figure 1(e) showcases a sample of normal CXR. Table 1 illustrates the allocation of training and testing data within the dataset. A data ratio of 8:2 is used for both training and testing data.

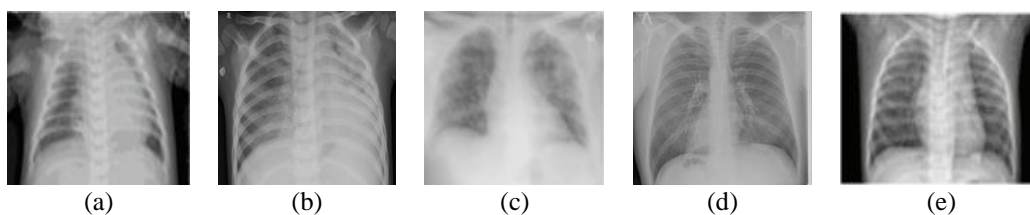


Figure 1. An example of bacterial pneumonia, viral pneumonia, COVID-19, tuberculosis, and normal CXR images; (a) bacterial pneumonia CXR, (b) viral pneumonia CXR, (c) COVID-19 CXR, (d) tuberculosis CXR, and (e) normal CXR

Table 1. The dataset applied in this study

Dataset/class	Bacterial pneumonia	Viral pneumonia	COVID-19	Tuberculosis	Normal	Total
Train	820	862	843	560	835	3,920
Test	206	216	211	140	209	982
Total	1,026	1,078	1,054	700	1,044	4,902

2.2. Data pre-processing

The image is adjusted to a resolution of 224×224 pixels in order to ensure uniformity in image size. The augmentation strategy is implemented during the pre-processing stage utilizing the Keras "ImageDataGenerator". Augmentation is necessary to enhance the diversity and quantity of data. Augmentation is used to enhance the variety of data, hence achieving a balanced dataset and optimizing the model. The batch size is configured to augment the overall data by 50. Furthermore, a rotation range of 900, a width shift range of 0.1, a height shift range of 0.1, and a zoom range of 0.05 are used. In addition, the rescale function is used to adjust the scale of the images by dividing them by 255. Next, a validation split of 0.2 is used to partition the data into separate training and validation sets. Table 2 displays the allocation of training data after the preprocessing stage.

Table 2. The dataset after preprocessing

Dataset/class	Bacterial pneumonia	Viral pneumonia	COVID-19	Tuberculosis	Normal	Total
Train	1220	1212	1243	1170	1235	6,080
Test	206	216	211	140	209	982
Total	1,426	1,428	1,454	1,310	1,444	7,062

2.3. Data modeling

This research devised a composite classification model by integrating CNN and BiLSTM. The study employs VGG19, InceptionV3, and Resnet50 as transfer learning CNN models. The CNN model is integrated with the BiLSTM model. Next, the CNN-BiLSTM model is contrasted with the standalone CNN model that does not have BiLSTM. This research utilizes Jupyter Notebook, Python 3.10, a Core i7 CPU, 16 GB of RAM operating at a speed of 3600MHz, and an Nvidia CUDA GPU for constructing the model.

The research utilized CNN-BiLSTM models, including VGG19-BiLSTM, InceptionV3-BiLSTM, and Resnet50-BiLSTM. The CNN-BiLSTM architecture consists of foundation models such as resnet50, VGG19, and InceptionV3. The base model of the CNN is enhanced by including a Flatten layer, which serves to transform the two-dimensional feature matrix into a one-dimensional vector. Then, it included two instances of BiLSTM with 64 units each. In order to mitigate overfitting, a dropout layer was used with a dropout rate of 0.3. Next, a flatten layer is added, followed by a batch normalization layer. The batch normalization layer is a layer used to expedite the training process of a model and enhance the stability and convergence of the model being trained. In addition, the fully connected layer (FCL) or dense layer is added with activation applied twice. Ultimately, the ultimate stratum of the CNN-BiLSTM framework produces a resultant picture that is classified into five categories using the SoftMax function. The code implementation of the Resnet50-BiLSTM architecture may be seen in Figure 2.

```

model_resnet50 = Sequential()
model_resnet50.add(base_model_resnet50)
model_resnet50.add(TimeDistributed(Flatten()))
model_resnet50.add(Bidirectional(LSTM(units=64, return_sequences=True)))
model_resnet50.add(Bidirectional(LSTM(units=64, return_sequences=False)))
model_resnet50.add(Dropout(0.3))
model_resnet50.add(Flatten())
model_resnet50.add(BatchNormalization())
model_resnet50.add(Dense(25, activation='relu'))
model_resnet50.add(Dense(5, activation="softmax"))

model_resnet50.summary()

```

Figure 2. Code implementation of Resnet50-BiLSTM architecture

This research presents a comparison between the CNN-BiLSTM model and the CNN model. The CNN models used in this investigation include VGG19, InceptionV3, and Resnet50. The architecture of a CNN consists of fundamental models such as VGG19, InceptionV3, and Resnet50. The base model of the CNN is augmented by a flatten layer, which is used to convert the feature matrix into a vector. Furthermore, the FCL or dense layer is included utilizing the Relu activation function with 128 neurons and 64 neurons. Additionally, a dropout layer was used to mitigate overfitting, with a dropout rate of 0.5. In order to get results for picture classification, a SoftMax activation layer is used at the final stage. The code implementation of the Resnet50 architecture is seen in Figure 3.

```

model_resnet50 = Sequential()
model_resnet50.add(base_model_resnet50)
model_resnet50.add(Flatten())
model_resnet50.add(Dense(128, activation='relu'))
model_resnet50.add(Dense(64, activation='relu'))
model_resnet50.add(Dropout(0.5))
model_resnet50.add(Dense(5, activation="softmax"))

model_resnet50.summary()

```

Figure 3. Code implementation of Resnet50 architecture

2.3. Hyperparameter tuning

During the hyperparameter tuning step, the most favorable values for the experimental scenario parameters are identified. The parameters used in this experiment are loss function, optimizer, batch size, model activation, and epoch. The loss function used in this work is categorical crossentropy. Adam works as an optimizer. The batch size used is 50. The number 25 serves as the epoch. Callback functions are used to mitigate undesired circumstances, such as the early halting function and the reduction of the learning rate. Early stopping is used to halt model training if there is no improvement in validation loss. The reduce learning rate function decreases the value of the learning rate if there is no improvement in the validation accuracy score.

3. RESULTS AND DISCUSSION

This research used six experimental categorization situations to classify lung illness using CXR data. The used experimental situations are VGG19-BiLSTM, InceptionV3-BiLSTM, Resnet50-BiLSTM, VGG19, InceptionV3, and Resnet50. Figure 4 illustrates a comparison of the accuracy of the research. The Resnet50-BiLSTM model outperforms other models in terms of accuracy. The Resnet50-BiLSTM model achieved a precision rate of 99.87%. The models that achieve the best accuracy are Resnet50, VGG19-BiLSTM, VGG19, InceptionV3-BiLSTM, and InceptionV3. The InceptionV3 model achieved a comparatively lower accuracy of 90.70% in comparison to the other models.

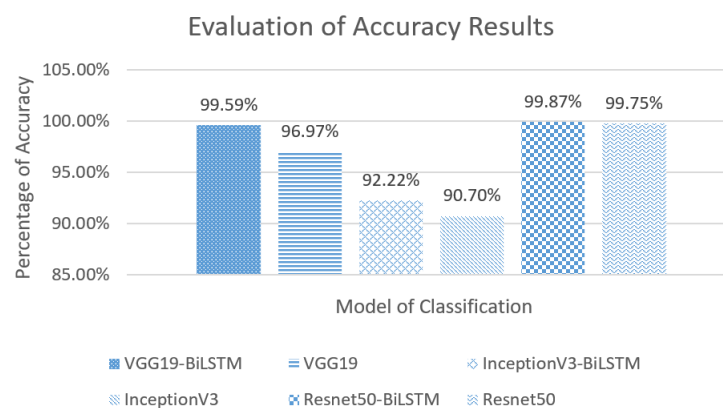


Figure 4. The comparison of accuracy results

The assessment of this research also incorporates the use of precision, recall, and F1-Measure. The objective of the assessment is to appraise the efficacy of the detection model by using COVID-19 CXR data. Table 3 presents the comparison of precision, recall, and F1-Measure. Upon comparing the precision, recall, and F1-Measure metrics, it is evident that Resnet50-BiLSTM outperforms other techniques by achieving the highest value. The precision, recall, and F1-Measure values for Resnet50-BiLSTM are 99.87%, 99.86%, and 99.86%, respectively. Subsequently, further models were introduced, including Resnet50, VGG19-BiLSTM, VGG19, InceptionV3-BiLSTM, and InceptionV3.

Table 3. The comparison of precision, recall, and F1-Measure

Model	Precision (%)	Recall (%)	F1-Measure (%)
VGG19-BiLSTM	99.59	99.58	99.58
Resnet50-BiLSTM	99.87	99.86	99.86
InceptionV3-BiLSTM	92.27	92.22	92.23
VGG19	97.00	96.98	96.98
Resnet50	99.75	99.75	99.75
InceptionV3	90.24	90.06	90.11

This research presents the confusion matrix data from the test to provide a detailed evaluation of the performance of each model. The Resnet50-BiLSTM model achieves the best accuracy by accurately detecting 1220 pictures in the bacterial pneumonia class and 1234 photos in the COVID-19 class. Within the standard class, the model has the capability to identify 1234 photos, with the exception of one image that is identified as a COVID-19 image. Out of the total of 1169 photos in the TB class, all were accurately diagnosed as tuberculosis except for one image that was mistakenly identified as COVID-19. In addition, 1206 photos were accurately categorized as viral pneumonia, whereas 3 images were classified as bacterial pneumonia and 3 images were identified as normal.

The InceptionV3 model has the worst accuracy performance among all the models. The model accurately identifies 1063 photos belonging to the bacterial pneumonia class. However, it mistakenly classifies 1 image as COVID-19, 2 images as normal class, and 153 images as viral pneumonia. In the COVID-19 classification, a total of 1145 photos were categorized as COVID-19, 5 images were classed as bacterial pneumonia, 69 images were classified as normal, 19 images were classified as TB, and 5 images were classified as viral pneumonia. Out of the total number of photos in the normal class, 1156 were accurately predicted as belonging to the normal class, while 79 images were mistakenly forecasted as belonging to other classes. Similarly, in the case of the TB class, 1073 photographs were accurately classified as belonging to the tuberculosis class, whereas 97 images were misclassified as belonging to other classes. In the viral pneumonia category, 1039 photos were accurately predicted whereas 173 images were inaccurately predicted. The confusion matrix model findings are shown in Figure 5. Figure 5 displays the model results of the confusion matrix which consists of; (a) VGG19-BiLSTM, (b) Resnet50-BiLSTM, (c) InceptionV3-BiLSTM, (d) VGG19, (e) Resnet50, and (f) InceptionV3.

This research demonstrates that the accuracy curve offers a comprehensive representation of the model's performance at each epoch. Figure 6 displays the accuracy curves for all models. Figure 6 displays the accuracy curve in models that consists of; (a) VGG19-BiLSTM, (b) Resnet50-BiLSTM (c) InceptionV3-BiLSTM, (d) VGG19, (e) Resnet50, and (f) InceptionV3. The Resnet50-BiLSTM model has a consistent and steady learning curve, demonstrating excellent levels of accuracy in both training and validation. The accuracy curve of the training data exhibits a consistent and gradual improvement from 0 to 25 epochs, reaching about 99%. The validation accuracy curve exhibits a rapid surge of 88% from epoch 0 to 1, followed by a gradual ascent until epoch 4. However, in epoch 5, the validation accuracy experiences a decline before rebounding in epoch 6. In addition, the validation accuracy rapidly increases and reaches around 95% by epoch 25. Contrary to the Resnet50-BiLSTM model curve, the inceptionV3 model has an accuracy curve that indicates underfitting. The accuracy curve for the training data exhibits a consistent and gradual rise, reaching a peak of 95%. However, the validation accuracy curve shows a fluctuating pattern of improvement. The validation accuracy declines at epochs 6 and 8, after which it gradually increases to about 80%.

The Resnet50-BiLSTM model demonstrated superior performance in comparison to the other models, as shown by the findings. The Resnet50-BiLSTM architecture is formed by combining the Resnet50 model with the BiLSTM model. The Resnet50 model has the capability to analyze localized responses within image data, enabling it to effectively extract features from CXR pictures in a parallel manner. The BiLSTM model excels in sequential data modelling, resulting in highly accurate data classification. Hence, the integration of Resnet50 and BiLSTM models capitalizes on the strengths of both models, resulting in superior

model performance compared to other models. The integration of CNN and BiLSTM models in this research yielded superior performance compared to the standalone CNN model that was not augmented with BiLSTM. The combination of the BiLSTM model with the CNN model has a positive impact on enhancing the performance of the COVID-19 classification model based on CXR Images.

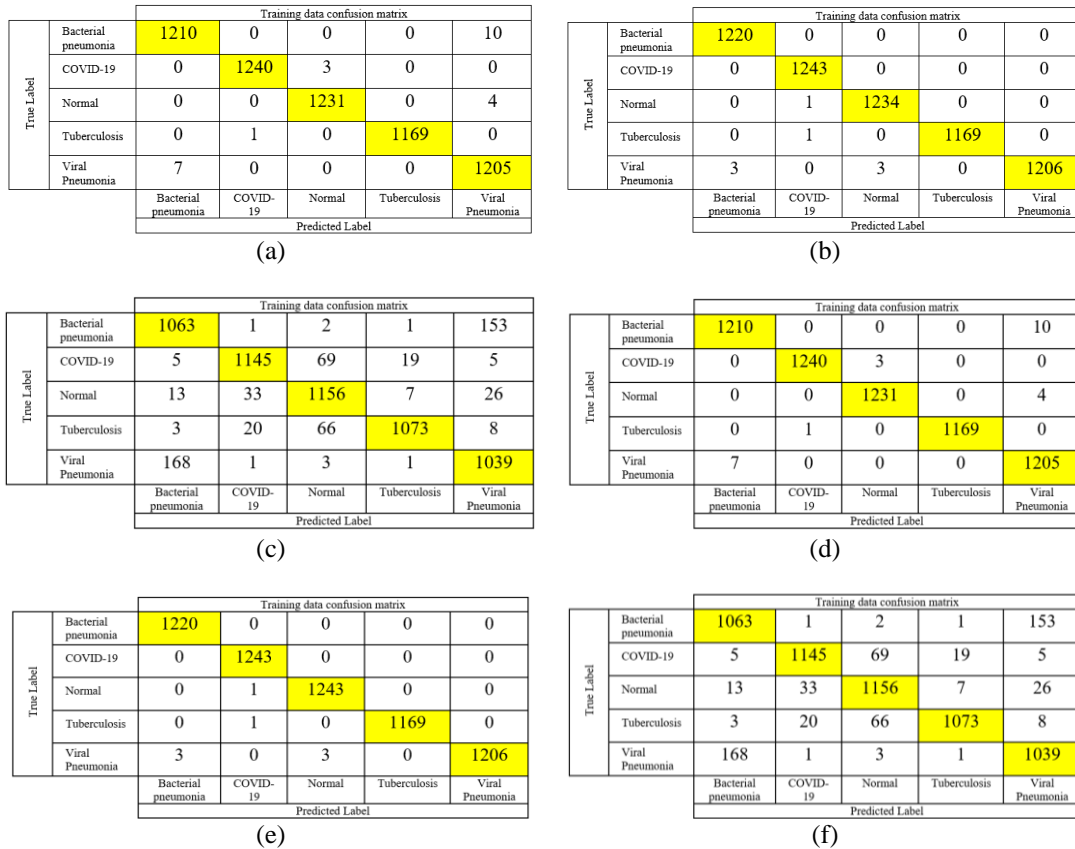


Figure 5. The model results of the confusion matrix; (a) VGG19-BiLSTM, (b) Resnet50-BiLSTM, (c) InceptionV3-BiLSTM, (d) Resnet50, (e) InceptionV3, and (f) VGG19

The CNN models examined in the present research are Resnet50, VGG19, and InceptionV3. The Resnet50 model outperformed other models, yielding superior outcomes. This is the case because of the Resnet50 design, which utilizes a shortcut connection concept to mitigate significant information loss during the training process. In order to improve the speed of the model, it is not feasible to only add layers while building the model architecture. As the depth of a network increases, there is an increased likelihood of encountering the vanishing gradient problem. This problem occurs when the gradient becomes exceedingly small, leading to decreased performance or accuracy [28]. Resnet introduced shortcut connections to mitigate the loss of important features during the convolution process.

The present study's analysis of model performance enhances performance results when compared to prior studies [29], [30]. The Resnet50-BiLSTM model achieves an accuracy of 93.3% and precision and recall rates of 93% each in identifying COVID-19. Prior studies using Resnet50-BiLSTM to identify pneumonia achieved an accuracy, precision, and recall of 99.15%, 99.18%, and 99.65% respectively. The findings of this research enhance the accuracy, precision, and recall of illness identification using CXR images, achieving rates of 99.87%, 99.87%, and 99.86% respectively. Therefore, this research improves the effectiveness of illness identification using CXR images. The reason for this is because the research used a broader dataset, namely consisting of CXR images of COVID-19, pneumonia, TB, and normal data, for the purpose of detecting lung diseases. The prior research did not use the TB dataset. This study also employs data augmentation approaches to address the issue of imbalanced data, hence enhancing data variety and optimizing the classification model. This work improves the efficacy of detecting lung disorders using CXR images.

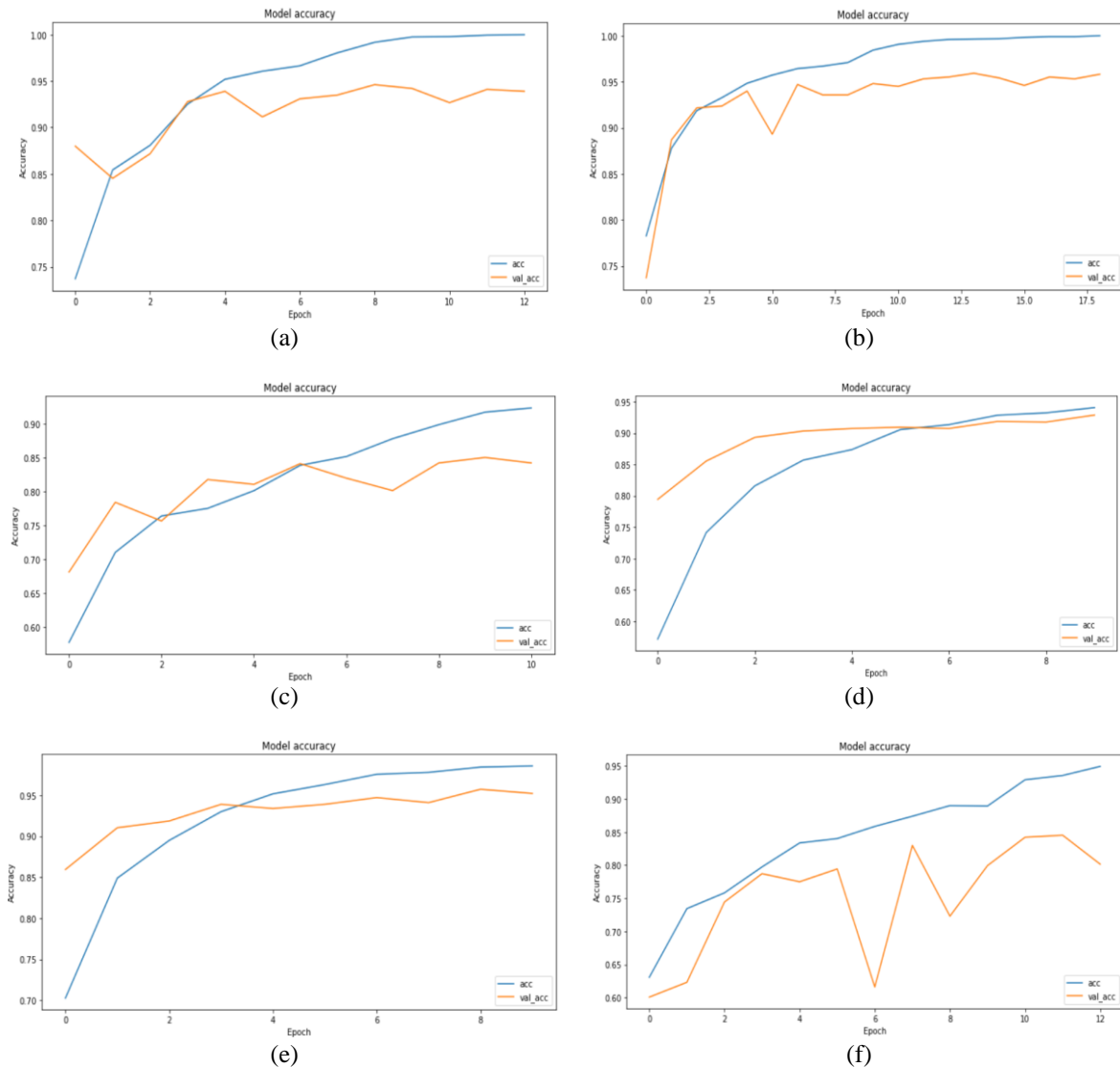


Figure 6. The accuracy curve in models; (a) VGG19-BiLSTM, (b) Resnet50-BiLSTM, (c) InceptionV3-BiLSTM, (d) VGG19, (e) Resnet50, and (f) InceptionV3

4. CONCLUSION

The research effectively categorized lung diseases by using a hybrid of CNN and BiLSTM models on CXR data. The CNN models used in this work are Resnet50, VGG19, and InceptionV3. This work used six different experimental scenarios to categorize data from CXR images. The scenarios are Resnet50-BiLSTM, VGG19-BiLSTM, InceptionV3-BiLSTM, Resnet50, VGG19, and InceptionV3. This study categorizes CXR into five distinct groups: Bacterial pneumonia, COVID-19, normal, TB, and Viral Pneumonia. The Resnet50-BiLSTM model outperforms other models in terms of accuracy, making it the optimal choice. The Resnet50-BiLSTM model achieved an accuracy rate of 99.87%. The models that achieve the best accuracy are Resnet50, VGG19-BiLSTM, VGG19, InceptionV3-BiLSTM, and InceptionV3. The research utilizes Precision, Recall, and F1-Measure to demonstrate that Resnet50-BiLSTM outperforms other methods by achieving the greatest value. Further research is needed to compare the performance of other transfer learning models, such as DenseNet or GoogleNet, with the transfer learning models used in this work. Moreover, additional investigation may be conducted to create a web-based application using the Django framework to classify lung disorders using CXR data.

ACKNOWLEDGEMENTS

We offer our gratitude to the Institute for Research and Community Service (LPPM) of Universitas Negeri Malang for their provision of research grant funds for the year 2024 based on contract letter number: 4.4.572/UN32.14.1/LT/2024. This report serves as a compulsory deliverable for the 2024 research grant and also functions as a means of ensuring responsibility for the funding. Gratitude is extended to colleague researchers who have contributed to the optimal outcomes of this study.




REFERENCES

- [1] F. Demir, A. Sengur, and V. Bajaj, "Convolutional neural networks based efficient approach for classification of lung diseases," *Health Information Science and Systems*, vol. 8, no. 1, p. 4, Dec. 2020, doi: 10.1007/s13755-019-0091-3.
- [2] S. H. Karaddi and L. D. Sharma, "Automated multi-class classification of lung diseases from CXR-images using pre-trained convolutional neural networks," *Expert Systems with Applications*, vol. 211, p. 118650, 2023, doi: 10.1016/j.eswa.2022.118650.
- [3] G. Zhang, L. Luo, L. Zhang, and Z. Liu, "Research Progress of Respiratory Disease and Idiopathic Pulmonary Fibrosis Based on Artificial Intelligence," *Diagnostics*, vol. 13, no. 3, p. 357, Jan. 2023, doi: 10.3390/diagnostics13030357.
- [4] J. Ma, Y. Song, X. Tian, Y. Hua, R. Zhang, and J. Wu, "Survey on deep learning for pulmonary medical imaging," *Frontiers of Medicine*, vol. 14, no. 4, pp. 450–469, 2020, doi: 10.1007/s11684-019-0726-4.
- [5] S. R. Nayak, D. R. Nayak, U. Sinha, V. Arora, and R. B. Pachori, "Application of deep learning techniques for detection of COVID-19 cases using chest X-ray images: A comprehensive study," *Biomedical Signal Processing and Control*, vol. 64, p. 102365, Feb. 2021, doi: 10.1016/j.bspc.2020.102365.
- [6] Y. Lecun, Y. Bengio, and G. Hinton, "Deep learning," *Nature*, vol. 521, no. 7553, pp. 436–444, 2015, doi: 10.1038/nature14539.
- [7] P. Chakraborty and C. Tharini, "Pneumonia and Eye Disease Detection using Convolutional Neural Networks," *Engineering, Technology and Applied Science Research*, vol. 10, no. 3, pp. 5769–5774, 2020, doi: 10.48084/etasr.3503.
- [8] M. Gil-Martín, J. M. Montero, and R. San-Segundo, "Parkinson's disease detection from drawing movements using convolutional neural networks," *Electronics (Switzerland)*, vol. 8, no. 8, p. 907, 2019, doi: 10.3390/electronics8080907.
- [9] D. E. Cahyani, F. F. Setyawan, A. D. Hariadi, L. T. Oktoviana, M. Yasin, and S. Wahyuningsih, "Detection of Pediatric Pneumonia using Convolutional Neural Networks and Vision Transformer," *Proceedings - IET 2023: 2023 International Conference on Electrical and Information Technology*, IEEE, pp. 180–184, 2023, doi: 10.1109/IET59852.2023.10335580.
- [10] A. Çınar, M. Yıldırım, and Y. Eroğlu, "Classification of pneumonia cell images using improved ResNet50 model," *Traitement du Signal*, vol. 38, no. 1, pp. 165–173, 2021, doi: 10.18280/TS.380117.
- [11] N. Dey, Y. D. Zhang, V. Rajinikanth, R. Pugalenth, and N. S. M. Raja, "Customized VGG19 Architecture for Pneumonia Detection in Chest X-Rays," *Pattern Recognition Letters*, vol. 143, pp. 67–74, 2021, doi: 10.1016/j.patrec.2020.12.010.
- [12] M. Rahimzadeh and A. Attar, "A modified deep convolutional neural network for detecting COVID-19 and pneumonia from chest X-ray images based on the concatenation of Xception and ResNet50V2," *Informatics in Medicine Unlocked*, vol. 19, p. 100360, 2020, doi: 10.1016/j.imu.2020.100360.
- [13] M. Nijati *et al.*, "Deep learning based CT images automatic analysis model for active/non-active pulmonary tuberculosis differential diagnosis," *Frontiers in Molecular Biosciences*, vol. 9, p. 1086047, Dec. 2022, doi: 10.3389/fmolb.2022.1086047.
- [14] M. Oloko-Oba and S. Viriri, "Ensemble of EfficientNets for the Diagnosis of Tuberculosis," *Computational Intelligence and Neuroscience*, vol. 2021, p. 9790894, Dec. 2021, doi: 10.1155/2021/9790894.
- [15] K. Nair, A. Deshpande, R. Guntuka, and A. Patil, "Analysing X-Ray Images to Detect Lung Diseases Using DenseNet-169 technique," *SSRN Electronic Journal*, 2022, doi: 10.2139/ssrn.4111864.
- [16] D. E. Cahyani, L. T. Oktoviana, A. D. Hariadi, F. F. Setyawan, and S. Setumin, "COVID-19 detection based on chest x-ray images using inception V3-BiLSTM," *AIP Conference Proceedings*, 2024, vol. 3049, no. 1, p. 20007, doi: 10.1063/5.0193859.
- [17] D. E. Cahyani, L. T. Oktoviana, A. N. Handayani, A. P. Wibawa, A. D. Hariadi, and F. F. Setyawan, "Comparison of Transfer Learning Models for COVID-19 Detection using Chest X-Ray Images," *Proceedings - International Conference on Informatics and Computational Sciences*, IEEE, 2022, pp. 95–100, doi: 10.1109/ICICoS56336.2022.9930532.
- [18] L. Wen, X. Li, and L. Gao, "A transfer convolutional neural network for fault diagnosis based on ResNet-50," *Neural Computing and Applications*, vol. 32, no. 10, pp. 6111–6124, 2020, doi: 10.1007/s00521-019-04097-w.
- [19] A. A. Ardakani, A. R. Kanafi, U. R. Acharya, N. Khadem, and A. Mohammadi, "Application of deep learning technique to manage COVID-19 in routine clinical practice using CT images: Results of 10 convolutional neural networks," *Computers in Biology and Medicine*, vol. 121, p. 103795, Jun. 2020, doi: 10.1016/j.combiomed.2020.103795.
- [20] X. Zhou *et al.*, "Partial Discharge Pattern Recognition of Transformer Based on Deep Learning," *Gaoya Dianqi/High Voltage Apparatus*, vol. 55, no. 12, 2019, doi: 10.13296/j.1001-1609.hva.2019.12.014.
- [21] Y. Chen *et al.*, "Stock Price Forecast Based on CNN-BiLSTM-ECA Model," *Scientific Programming*, vol. 2021, pp. 1–20, 2021, doi: 10.1155/2021/2446543.
- [22] W. Meng, Y. Wei, P. Liu, Z. Zhu, and H. Yin, "Aspect Based Sentiment Analysis with Feature Enhanced Attention CNN-BiLSTM," *IEEE Access*, vol. 7, pp. 167240–167249, 2019, doi: 10.1109/ACCESS.2019.2952888.
- [23] J. Xu, Y. Zhang, and D. Miao, "Three-way confusion matrix for classification: A measure driven view," *Information Sciences*, vol. 507, pp. 772–794, 2020, doi: 10.1016/j.ins.2019.06.064.
- [24] M. E. H. Chowdhury *et al.*, "Can AI Help in Screening Viral and COVID-19 Pneumonia?," *IEEE Access*, vol. 8, pp. 132665–132676, 2020, doi: 10.1109/ACCESS.2020.3010287.
- [25] T. Rahman *et al.*, "Exploring the effect of image enhancement techniques on COVID-19 detection using chest X-ray images," *Computers in Biology and Medicine*, vol. 132, Qeios Ltd, 2021, doi: 10.1016/j.combiomed.2021.104319.
- [26] O. M. Dalvil, March 26, 2024, "Lungs Disease Dataset (4 types)," IEEE Dataport, doi: 0.21227/c5ax-qj62.
- [27] T. Rahman *et al.*, "Reliable tuberculosis detection using chest X-ray with deep learning, segmentation and visualization," *IEEE Access*, vol. 8, pp. 191586–191601, 2020, doi: 10.1109/ACCESS.2020.3031384.
- [28] N. Alsharman and I. Jawarneh, "GoogLeNet CNN neural network towards chest CT-coronavirus medical image classification," *Journal of Computer Science*, vol. 16, no. 5, pp. 620–625, 2020, doi: 10.3844/JCSP.2020.620.625.
- [29] D. E. Cahyani, A. D. Hariadi, F. F. Setyawan, L. Gumila, and S. Setumin, "COVID-19 classification using CNN-BiLSTM based on chest X-ray images," *Bulletin of Electrical Engineering and Informatics*, vol. 12, no. 3, pp. 1773–1782, 2023, doi: 10.11591/eei.v12i3.4848.


- [30] D. E. Cahyani, A. D. Hariadi, F. F. Setyawan, L. Gumilar, and S. Setumin, "Classification of pediatric pneumonia using ensemble transfer learning convolutional neural network," *Bulletin of Electrical Engineering and Informatics*, vol. 13, no. 5, pp. 3411–3417, 2024, doi: 10.11591/eei.v13i5.7825.

BIOGRAPHIES OF AUTHORS






Denis Eka Cahyani    holds a Bachelor of Computer Science (S. Kom.) in Computer Science, Master of Computer Science (M.Kom.) in Computer Science, Universitas Indonesia in 2015 besides several professional certificates and skills. She holds a Bachelor of Informatics degree from Universitas Sebelas Maret, Indonesia in 2013. She is currently lecturing with the Department of Mathematics at Universitas Negeri Malang, Malang, Indonesia. She is a member of the Engineers and the Institute of Electrical and Electronics Engineers (IEEE) Indonesia Section. Her research areas of interest include data science, natural language processing, and artificial intelligent. She can be contacted at email: denis.eka.cahyani.fmipa@um.ac.id.






Lucky Tri Oktoviana    received the Bachelor of Mathematics (S.Si.) degree in Mathematics Department from Institut Teknologi Sepuluh November (ITS), Indonesia, in 1992 and the Master of Computer Science (M.Kom.) degree in Computer Science, Institut Teknologi Sepuluh November (ITS), Indonesia in 2002. Currently, she is a lecturer at Department of Mathematics, Universitas Negeri Malang, Indonesia. Her interest research is mathematics computation, artificial intelligence, information system, and database. She can be contacted at email: lucky.tri.fmipa@um.ac.id.






Mohamad Yasin    received the Bachelor of Computer Science (S.Kom.) degree in Computer Science from Institut Teknologi Sepuluh November (ITS), Indonesia, in 1997 and the Master of Computer Science (M.Kom.) degree in Computer Science, Institut Teknologi Sepuluh November (ITS), Indonesia in 2004. Currently, he is a lecturer at Department of Mathematics, Universitas Negeri Malang, Indonesia. His interest research is mathematics computation, artificial intelligence, information system, and database. She can be contacted at email: mohamad.yasin.fmipa@um.ac.id.






Sapti Wahyuningsih    received the Bachelor of Mathematics (Dra.) degree in Mathematics from Universitas Gajahmada, Indonesia in 1987, and the Master of Mathematics (M.Si.) degree in Mathematics, Institut Teknologi Bandung (ITB), Indonesia in 1994. Currently, she is a lecturer at Department of Mathematics, Universitas Negeri Malang, Indonesia. Her interest research is applied mathematics. She can be contacted at email: sapti.wahyuningsih.fmipa@um.ac.id.






Dionixius    is currently student in department of Mathematics at Universitas Negeri Malang, Malang, Indonesia since 2020. He has attended Bangkit Academy by Google, GoTo Traveloka Machine Learning cohort. His research areas of interest include machine learning, and deep learning. He can be contacted at email: dionixius.2003126@students.um.ac.id.



Ranti Maulidaningsih    is currently student in department of Mathematics at Universitas Negeri Malang, Malang, Indonesia since 2020. She has attended Bangkit Academy by Google, GoTo Traveloka Machine Learning cohort. Her research areas of interest include machine learning, and deep learning. He can be contacted at email: ranti.maulidaningsih.2003126@students.um.ac.id.



Samsul Setumin    received the B.Eng. degree (Hons.) in electronic engineering from the University of Surrey, in 2006, and the M.Eng. degree in electrical-electronic and telecommunication from the Universiti Teknologi Malaysia, in 2009. He obtained his Ph.D. degree from Universiti Sains Malaysia in 2019 in the imaging field. Since 2010, he has been a Lecturer with the Universiti Teknologi MARA, Malaysia. He was a Test Engineer with Agilent Technologies (M) Sdn. Bhd., and Intel Microelectronics (M) Sdn. Bhd., for a period of one year. His research interests include computer vision, image processing, pattern recognition, and embedded system design. He can be contacted at email: samsuls@uitm.edu.my.